Article

Chinese Science Bulletin

Oceanology

November 2010 Vol.55 No.32: 3709–3717
doi: 10.1007/s11434-010-4172-6

Warming magnitude of Indonesian Throughflow during the penultimate deglaciation (Termination II) and its relationship with climate change in high-latitude regions

TIAN CuiCui* & TIAN Jun*

State Key Laboratory of Marine Geology, Tongji University, Shanghai 200092, China

Received April 23, 2010; accepted August 3, 2010

The tropical oceans are important source areas for global heat and water vapor transport, and changes in tropical sea surface temperature (SST) will have important impacts on high-latitude and global climate change. It is crucial to establish the precise phase relationship between tropical and high-latitude climate variability to gain insight into the mechanisms of global climate change. Here, we present multi-proxy records across the penultimate deglaciation (Termination II) from sediment Core SO18459, which is located in the outflow area of the Indonesian Throughflow (ITF) of the Timor Sea. These proxy records include planktonic and benthic foraminifera $\delta^{18}O$, planktonic foraminifera *G. ruber* Mg/Ca-derived SST, and $\delta^{18}O_w$ of sea surface water. The Mg/Ca-SST records indicate a warming of 4.1°C in the Timor Sea over Termination II, which is in phase with decrease in planktonic and benthic $\delta^{18}O$. Our results suggest that at millennial timescales, climate change of the tropical oceans is synchronous with high-latitude ice volume changes. Furthermore, warming of the Timor Sea is almost simultaneous with warming of the Antarctic, suggesting a rapid heat transfer from the tropics to the Antarctic via the atmosphere and/or ocean circulations. The *G. ruber* $\delta^{18}O$ and SST records of Core SO18459 show a marked YD-like event during Termination II, which is probably caused by decrease in Australian rainfall or strengthening of the Western Pacific Warm Pool. However, a similar YD-like event is not observed in East Asian rainfall records. This discrepancy indicates that different tropical climate systems may have different responses to the same forcing, such as El Niño Southern Oscillation. A similar YD-like event is observed in the global benthic foraminiferal $\delta^{18}O$ records during Termination II, implying teleconnection of millennial scale climate change between the tropical regions and high latitudes.

Indonesian Throughflow, Termination II, tropic sea surface temperature, high-latitude, phase relationship

Citation: Tian C C, Tian J. Warming magnitude of Indonesian Throughflow during the penultimate deglaciation (Termination II) and its relationship with climate change in high-latitude regions. Chinese Sci Bull, 2010, 55: 3709–3717, doi: 10.1007/s11434-010-4172-6

The Indo-Pacific Warm Pool (IPWP) provides heat and water vapor for ice sheet growth, and is the main source of global heat transport to the high latitudes through thermohaline circulation (THC) [1,2]. Recent studies have suggested that tropical sea surface temperatures (SSTs) increased by 4°C [3–5] during the penultimate deglaciation (Termination II), and planktonic foraminiferal $\delta^{18}O$, which indicates ice volume changes, lagged the Mg/Ca-SST changes by 2000–3000 a [3–6]. Such great changes in SST have had a significant role in regulating global climate change [6,7]. Because planktonic foraminiferal $\delta^{18}O$ relates largely to high-latitude ice volume changes, the distinct phase difference has raised a debate over whether climate change is triggered in the high-latitudes or tropics [3–8]. However, some studies have suggested that there was no distinct phase difference between planktonic foraminiferal $\delta^{18}O$ and Mg/Ca-SST, and tropical SST changed synchronously with ice volume (benthic $\delta^{18}O$) during deglaciations [4]. It is therefore crucial to establish the precise phases between tropical and high-latitude climate variability to gain insight

*Corresponding authors (email: cct1234@163.com; tianjun@tongji.edu.cn)

into the mechanisms of global climate change [9].

The Indonesian Throughflow (ITF) connects the upper water masses of the Western Pacific and the Indian Ocean, and is an important part of the surface warm current of the global thermohaline circulation. The ITF plays an important role in heat and water vapor transport from the tropics to the high latitudes. It is affected by the Asian monsoon and El Niño [10–12] and also plays a role in amplifying the signals of global climate change.

A previous multi-proxy investigation by Visser et al. [3] on Core MD9821-62, located in the Timor Sea, estimated that foraminiferal δ^{18}O (which indicates global ice volume changes) lagged the Mg/Ca-derived SST changes by 2000–3000 a, indicating that the tropical western Pacific region warmed before the melting of Northern Hemisphere ice sheets. In contrast, Xu et al. [4] found that SSTs in the Timor Sea had been in phase with both planktonic and benthic foraminiferal δ^{18}O over Termination II. The phase relationship between SST and planktonic δ^{18}O in the Timor Sea is still poorly established. To better understand this phase relationship, we present here multi-proxy records including planktonic and benthic foraminifera δ^{18}O, *Globigerinoides ruber* Mg/Ca-derived SST and $\delta^{18}O_w$ of sea surface water from sediment Core SO18459 located in the outflow area of the ITF, to reconstruct the history of ITF variability in Termination II and to investigate the phase relationship of climate change between the tropical oceans and high-latitude regiens.

1 Materials and methods

Sediment Core SO18459 (8°29.997'S, 128°10.002'E; 1743 m water depth) was collected by sonne-185 "VITAL" in 2005, and is located in the outflow area of the ITF in the Timor Sea (Figure 1). The core was located close to previous Cores MD9821-62 and MD01-2378, and each is located at different branches of the ITF. 192 samples were taken at 2-cm intervals between depths 1200 to 1584 cm in Core SO18459, which has an overall length of 1599 cm.

1.1 Stable carbon and oxygen isotopes

Stable carbon and oxygen isotope measurements were made following standard procedures [14] with a Finnigan MAT 252 mass spectrometer at the State Key Laboratory of Marine Geology of Tongji University. Samples were dried at 50°C and soaked in water for 1–2 d, then washed through a 63-μm sieve, and the >63 μm size fraction was dried again at 50°C. Well-preserved, clean, and unbroken species of *Globigerinoides ruber* (300–360 μm, white, 12 tests) and *Cibicidoides wuellerstorfi* (≥2 tests) without obvious signs of dissolution were processed for stable carbon and oxygen isotopes. Foraminiferal shells were cleaned three times in 99.7% alcohol in an ultrasonic bath at a frequency of 40 kHz, and dried at 60°C for 5 h. Stable carbon and oxygen isotope measurements were made with the Finnigan MAT 252 mass

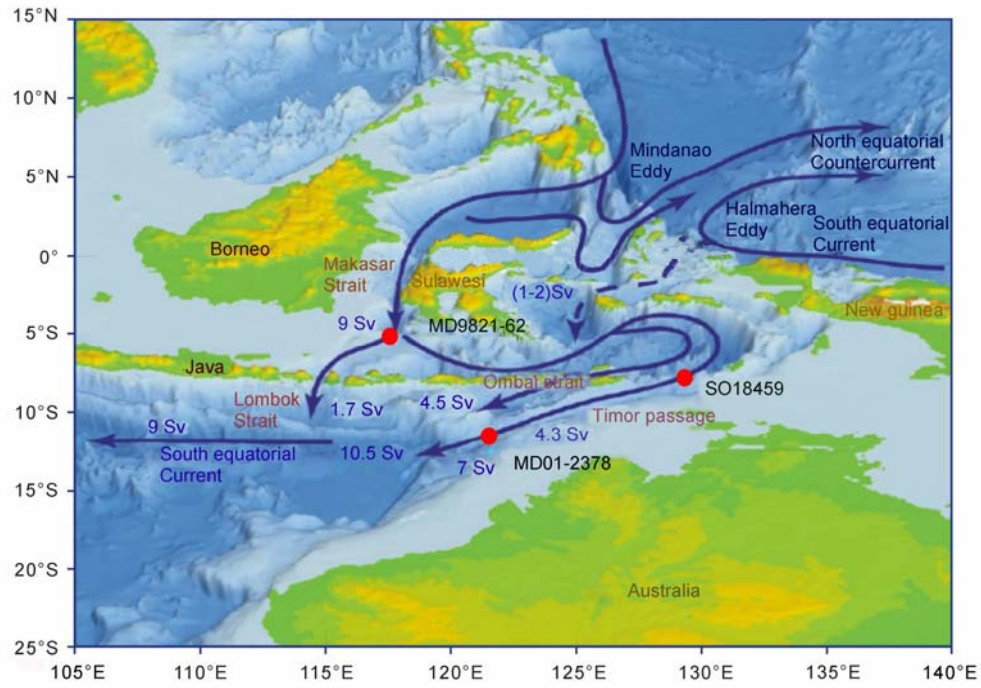

Figure 1 Location of Cores SO18459, MD01-2378 [4,5] and MD9821-62 [3] (red solid circles). Green and yellow colors indicate continents. Dark blue is continental slopes and sea basins, and light blue represents shallow continental shelves. Dark blue arrows indicate the main ITF pathways. Modified from Kuhnt et al. [13].

spectrometer equipped with an automated carbonate system (Type III). The samples were reacted in a common acid bath of 100% phosphoric acid at 70°C. The evolved CO_2 gas was then analyzed on the mass spectrometer. The mean external error and reproducibility of carbonate standards were better than ±0.07‰ and ±0.04‰ for $\delta^{18}O$ and $\delta^{13}C$, respectively. Results were calibrated using the National Institute of Standards and Technology (Gaithersburg, MD, USA) carbonate isotope standard NBS 19 and 18, and are reported on the Peedee belemnite (PDB) scale.

1.2 Mg/Ca paleothermometry

The Mg/Ca ratio in *G. ruber* was determined on an inductively coupled plasma-atomic emission spectrophotometer (ICP-AES) at the State Key Laboratory of Marine Geology, Tongji University. Approximately 40 shells (white, 0.25–0.35 mm shell diameter, uncontaminated) of *G. ruber* were processed using the following procedure. First, the samples were weighed and placed on a clean glass slide. The foraminifer shells were gently crushed with another clean glass slide, ensuring that all chambers were fully exposed. After removing impurities, the foraminifer fragments were transferred into transparent plastic tubes. Second, the foraminifer fragments were covered with deionized water (DI H_2O), sonicated for ~30 s, then the supernatant was siphoned off using a micropipette. These steps were repeated three times with DI H_2O, twice with methanol, and then once with DI H_2O to remove the methanol. Third, to remove oxidizing material, 100 μL of chemical solution A (750 μL hydrazine, 10 mL ammonia and 10 mL citric acid of 0.5 g/L) was added. The sample was then cleaned with DI H_2O three times to remove the hydrazine. After this, 250 μL of chemical solution B (30 mL 0.1 g/L NaOH and 300 μL 30% H_2O_2) was added to remove organic matter. The samples were capped and placed in a boiling water bath for 10 min, then sonicated twice for 2 s. To remove the oxidizing solution B, the samples were rinsed three times with DI H_2O, and then transferred to new, acid-cleaned microcentrifuge tubes. The cleaned samples were leached with 100 μL of weak acid of 0.001 g/L HNO_3 and rinsed with DI H_2O twice. Finally, the samples were processed on ICP-AES following the procedure of Lea et al. [6]. The spectral lines of Ca3158, Mg2852, Fe2599, Mn2593 and Sr4077 were detected. The values of Fe, Mn and Sr were used to evaluate the effectiveness of sample cleaning [15] to detect influences of foraminiferal Fe and Mn oxides coverings layer on the ratio of Mg/Ca.

1.3 $\delta^{18}O_w$ of sea surface water reconstruction

$\delta^{18}O_w$ ($\delta^{18}O$ of sea surface water) relates to seawater salinity and global ice volume or global sea-level change [16]. Shackleton [17] described the quantitative relationship between $\delta^{18}O$ of foraminifer shells and seawater $\delta^{18}O$ temperature. Bemis et al. [18] later developed the equation: $\delta^{18}O_w$ (VSMOW) = 0.27 + T (°C) − 16.5 +4.8 ×$\delta^{18}O_{calcite}$ (VPDB)/4.8. Xu et al. [4] applied this equation to the top sample of Core MD01-2378. The calculated $\delta^{18}O_w$ values were between the measured $\delta^{18}O_w$ values of –0.5‰ in the Western Pacific Warm Pool (WPWP) and the measured $\delta^{18}O_w$ values of 0.6‰ in the upper 300 m of the eastern Indian Ocean.

2 Results

2.1 Age model

MIS 6–5e is beyond the time range of AMS ^{14}C dating. Thus we developed a new age model for MIS 6–5 e which follows the specific benthic oxygen isotope stratigraphy. Benthic $\delta^{18}O$ records from the global oceans show nearly the same curves from at least the Pliocene until now, representing global ice volume change. Based on the benthic $\delta^{18}O$ records from ODP site 677, Shackleton et al. [19] developed an astronomically tuned timescale for the past 2 Ma, providing an age standard to compare with other deep sea sites. The newly developed LR04 [20] timescale is based on an integration of 57 benthic $\delta^{18}O$ records from globally distributed deep sea sites, which covers the past 5.3 Ma and has been used widely by many researchers. It is very common in paleoceanographic studies to establish an age model based on the comparison of benthic $\delta^{18}O$ records from the studied sites with the stacked $\delta^{18}O$ chronology of LR04. On orbital and millennial timescales, the duration of deglaciation is relatively short, and the beginning, peak and end points of deglaciation are usually chosen as reference points. In addition, other isotope tie points, for example the peak and the transition points of benthic $\delta^{18}O$ curves, are also used as reference points.

In this study, our discussion only focuses on Termination II. An initial stratigraphy was obtained based on the color reflectance (L^*) records of Core SO18459. In the Pacific and Indian Ocean, the L^* value of deep-sea cores represents brightness and can be correlated directly to change in calcium carbonate content. In the late Pleistocene, the color reflectance records are consistent with glacial-interglacial cycles of foraminifera $\delta^{18}O$. In recent decades, the initial shipboard stratigraphy of the sediment cores was obtained by matching magnetic susceptibility and lightness records with well-known age models such as SPECMAP for all IMAGES and Sonne cruises. In our study, the L^* records of Core SO18459 show clearly that the depth interval 1200–1584 cm of Core SO18459 corresponds to MIS 5–6, which covers the whole Termination II (Figure 2). We correlate the benthic $\delta^{18}O$ record of Core SO18459 to that of the ''LR04'' stack [20] chronology to obtain an age model, as shown in Figure 2.

Seven rapidly changing and extreme points in the benthic δ^{18}O record of Core SO18459 were chosen as tie points, and were then assigned ages by comparison with the LR04 benthic δ^{18}O record (Table 1 and Figure 2). For the few samples above 1232.5 cm and below 1536.5 cm, we extrapolated the ages by assuming a constant sedimentation rate. The depth 1200–1584 cm covers the period from ca. 93 to 152 ka BP. In our age model Termination II is from ca. 128 to 135 ka BP. The average sedimentation rate is 6.25 cm ka^{-1} and the average temporal sampling resolution is ~320 a.

2.2 Stable oxygen isotopes

Both planktonic and benthic foraminifer δ^{18}O records show similar trends, except for in MIS 5.4 (Figure 4). *G. ruber* δ^{18}O shows large values around –1.15‰ during MIS 6. During Termination II, *G. ruber* δ^{18}O varies from –1.05‰at ca. 135 ka BP to –2.47‰ ca. 128 ka BP, with a decrease

Table 1 Tie points of Core SO18459

Station	Depth (cm)	Age (ka BP)	Tuning curve	Comment
18459	1200.5	92.88	LR04 stack	Based on the sedimentation rate between 1232.5 cm and 1282.5 cm [a)]
18459	1232.5	98	LR04 stack	An extreme point of MIS 5.3
18459	1282.5	106	LR04 stack	MIS 5.3/5.4
18459	1360.5	112	LR04 stack	An extreme point of MIS 5.4
18459	1416.5	117	LR04 stack	MIS 5.4/5.5
18459	1476.5	125	LR04 stack	An extreme point of MIS 5.5
18459	1516.5	135	LR04 stack	The bottom of Termination II
18459	1536.5	140	LR04 stack	An extreme point of MIS 6
18459	1584.5	152	LR04 stack	Based on the sedimentation rate between 1516.5 cm and 1536.5 cm [b)]

a), b) Linear extension is based on the sedimentation rate of neighboring points.

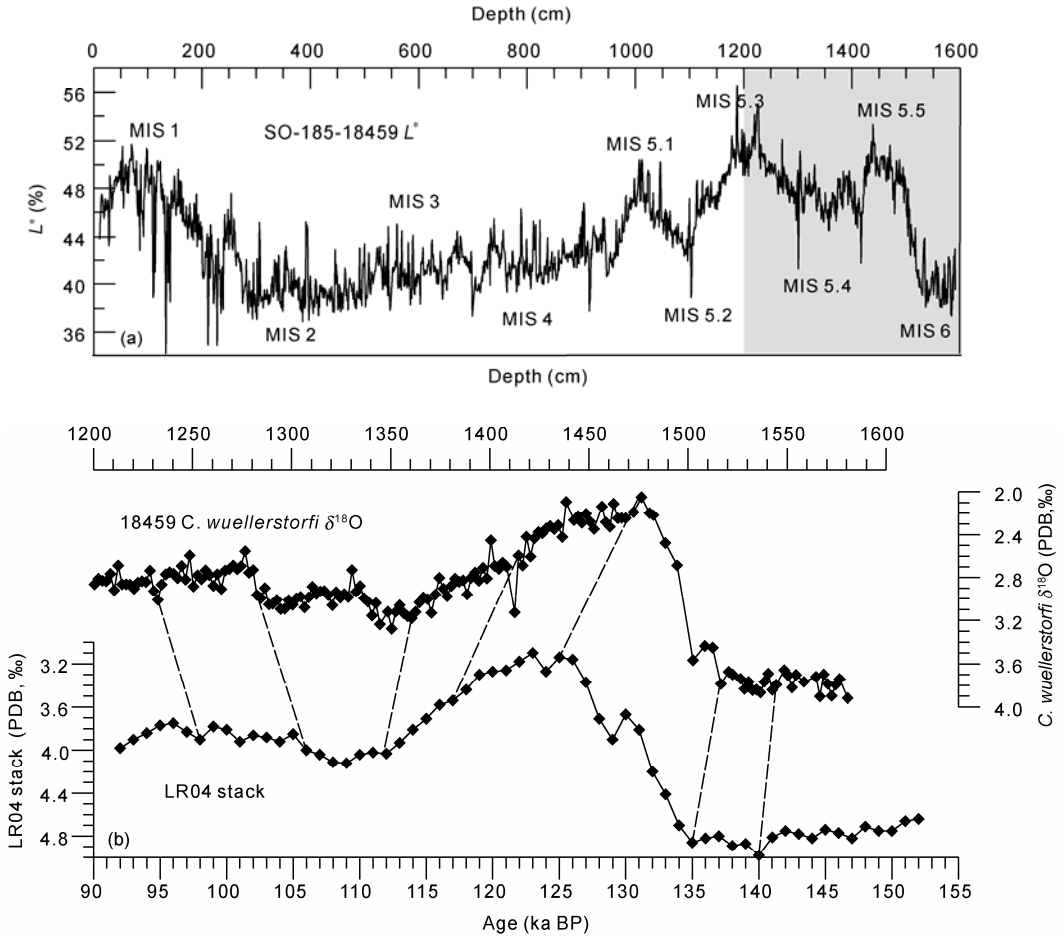

Figure 2 (a) Color reflectance (L^*) records of Core SO18459. The shaded zone is the period of our study. (b) Our age model. The benthic *C. wuellerstorfi* δ^{18}O record of Core SO18459 was correlated to the "LR04" stack [20] chronology, the black dotted line represents the tie points.

of ~1.42‰. A short increase of *G. ruber* δ^{18}O of ~0.35‰ occurs between ca. 130.5 ka BP and ca. 133.5 ka BP, and after that *G. ruber* δ^{18}O decreases rapidly. A minimum plateau of *G. ruber* δ^{18}O occurs between ca. 128 and 117 ka BP with an average value of –2.65‰. After ca. 117 ka BP, *G. ruber* δ^{18}O increases. There is no distinct difference in *G. ruber* δ^{18}O between MIS 5.4 (stadial) and MIS 5.3 (interstadial).

Benthic *C. wuellerstorfi* δ^{18}O records are similar to planktonic *G. ruber* δ^{18}O records. Before Termination II, the values of benthic δ^{18}O are high although fluctuate slightly, and are ~3.78‰ on average. Between ca. 135 and 128 ka BP the values of benthic δ^{18}O decrease rapidly by 1.31‰. In contrast to the *G. ruber* δ^{18}O record, a short increase of *C. wuellerstorfi* δ^{18}O values does not occur between ca. 130.5 and 133.5 ka BP. The whole of MIS 5.5 is characterized by a plateau of minimum *G. ruber* δ^{18}O values, with an average value of 2.3‰. After an increase in *C. wuellerstorfi* δ^{18}O values in MIS 5.4, a maximum value of ~3.28‰ occurs until ca. 111 ka BP, followed by an obvious decrease in values during MIS 5.3.

2.3 Mg/Ca-derived SST during Termination II

We use the equation developed by Anand et al. [21] from a 6-year sediment trap time series in the Sargasso Sea to calculate SST from the Mg/Ca ratios of *G. ruber*: Mg/Ca (mmol mol^{-1}) = 0.38 (±0.02) exp 0.090 (±0.003) × SST (°C). The accuracy of this equation is ±1.2°C. In the Timor Sea, the equation (Mg/Ca (mmol mol^{-1}) = 0.30 $e^{0.089 \times T\,(°C)}$) developed by Lea et al. [6] and the equation (Mg/Ca (mmol mol^{-1}) = 0.38 $e^{(0.09 \times (\text{SST } (°C)) - 0.61 \times \text{core depth (km)} - 1.6°C))}$) developed by Dekens et al. [22] overestimate the SST of Core SO18459 due to dissolution effects of foraminifer shells (Figure 3). To assess the validity of the equation developed by Anand et al. [21] in this region, Xu et al. [4] measured Mg/Ca ratios of foraminifers picked from 12 multicore core top samples from six stations along a depth transect between 560 and 2320 m. The calculated SST and the upper thermocline temperature based on the equation developed by Anand et al. [21] fall into the range of observed average SST and the upper thermocline temperatures that occur during summer in this region.

In our study, SST of Core SO18459 was calculated using the equation developed by Anand et al. [21], as shown in Figure 3. SST is low during MIS 6 and then increases rapidly during Termination II. At MIS 5.5, SST reaches the warmest value of ~28.9°C. After ca. 124 ka BP, SST gradually decreases until ca. 111 ka BP and then increases again. The magnitude of warming recorded in Core SO18459 is ~4.1°C during Termination II, which is similar to the value of ~4.1±0.6°C estimated by Visser et al. [3] for Core MD9821-62 (4°41.33′S, 117°54.17′E; 1855 m water depth) and to the value of ~4.2°C estimated by Xu et al. [4] for Core MD01-2378 (13°4.95′S, 121°47.27′E; 1783 m water depth).

2.4 δ^{18}O of sea surface water ($\delta^{18}O_w$)

The δ^{18}O of sea surface water ($\delta^{18}O_w$) is calculated using the equation developed by Bemis et al. [18], as shown in Figure 4. During MIS 6 and early Termination II, the $\delta^{18}O_w$ shows high values with small amplitude fluctuation. At the beginning of Termination II, the average $\delta^{18}O_w$ is ~0.95‰, indicating higher salinity. The $\delta^{18}O_w$ then decreases rapidly, reaching the minimum value of –0.16‰ at ca. 127.5 ka BP.

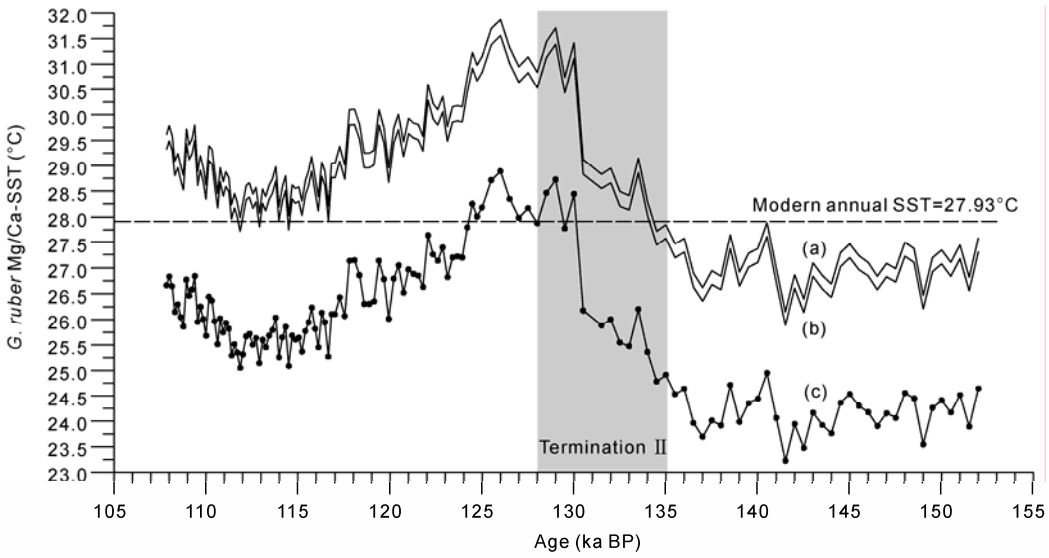

Figure 3 *G. ruber* Mg/Ca-SST calculated using different equations. Mg/Ca-SST developed by Lea et al. [6] (a); Mg/Ca-SST developed by Dekens et al. [22] (b); Mg/Ca-SST developed by Anand et al. [21] (c). Dotted line is the modern annual SST from the upper 50 m of water in this core location (World Ocean Atlas, 2005 data).

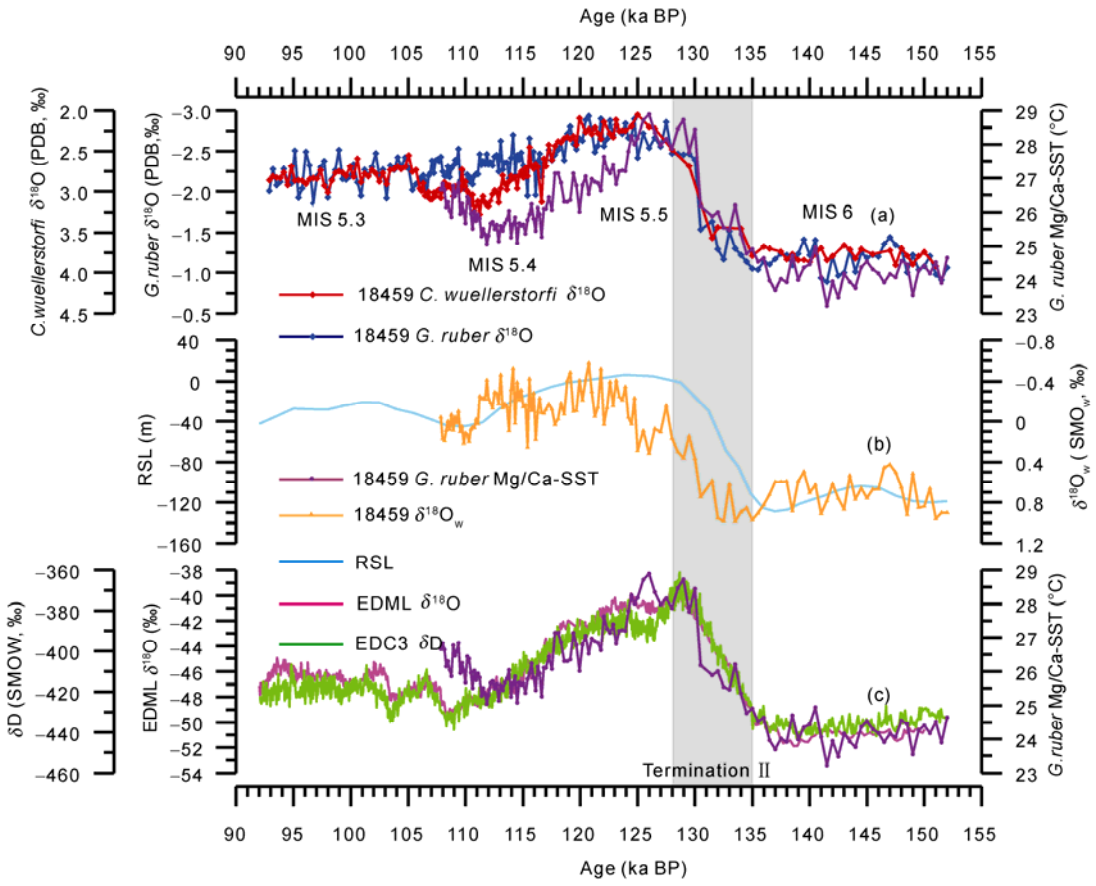

Figure 4 Comparison of different records. (a) planktonic δ^{18}O (blue), benthic δ^{18}O (red) and Mg/Ca-SST (purple) from Core SO18459; (b) surface seawater $\delta^{18}O_w$ from Core SO18459 (yellow) and global sea level change [23] (light blue); (c) Mg/Ca-SST (purple) from Core SO18459, EDC3 δD record (green) and EDML δ^{18}O record (pink) [25].

The overall decrease in $\delta^{18}O_w$ of Core SO18459 is ~1.1‰ for the whole of Termination II, which is slightly larger than the ice volume effect of ~1‰ as estimated by Waelbroeck et al. [23]. We accordingly consider that the surface seawater $\delta^{18}O_w$ of Core SO18459 represents global ice volume change.

3 Discussion

3.1 High- and low-latitude climate changes

The Mg/Ca-SST indicates that the warming magnitude of the ITF during Termination II is ~4.1°C in Core SO18459, which is consistent with Cores MD9821-62 and MD01-2378 [3,4]. In contrast to other studies, planktonic or benthic δ^{18}O did not lag the Mg/Ca-SST changes by 2000–3000 a [3,4,24]. Rather, changes in SST over Termination II are synchronous with planktonic and benthic δ^{18}O records at millennial timescales. Because benthic δ^{18}O reflects largely high-latitude ice volume changes, this phase relationship indicates that tropical sea surface water warming and high-latitude ice sheet melting are almost synchronous.

Visser et al. [3] explained the lag of planktonic δ^{18}O relative to SST by 2000–3000 a observed in Core MD9821-62, by proposing that the tropical western Pacific region warmed before melting of Northern Hemisphere ice sheets during deglaciation. Change in global ice volume contributes only to a part of the changes in *G. ruber*. In addition to global ice volume, local surface seawater temperature and salinity are also important factors influencing *G. ruber*. The phase lag suggested by Visser et al. [3] could be explained to some extent by local variability in the tropical climate. The surface seawater of Makassar Strait could be influenced by local rainfall because surface salinity of this area is influenced strongly by continental runoff from Borneo (Figure 1). A lag of *G. ruber* δ^{18}O relative to SST in the early phase of Termination II could be caused by changes in surface water salinity. A northward shift of the Inter-Tropical Convergence Zone (ITCZ) during the boreal summer could result in decreases in monsoonal rainfall over Borneo, which then changes regional surface seawater salinity and δ^{18}O of *G. ruber* [4].

In Core SO18459, Mg/Ca-SST and planktonic δ^{18}O change synchronously, which is consistent with Core MD01-2378 [4,5]. In addition, change in $\delta^{18}O_w$ from Core SO18459 is ~1.1‰ during Termination II, which approximates the average $\delta^{18}O_w$ of ~1‰ caused by global ice volume change

[23]. We infer that surface seawater salinity has very small effects on planktonic δ^{18}O record during Termination II in the Timor Sea. These results do not support the notion that warming of the tropical sea surface water leads to melting of the northern hemisphere ice sheet during deglaciations [3].

The effect of sea surface salinity on planktonic δ^{18}O varies through time because of local climate change. Therefore, the benthic δ^{18}O record is more reliable in representing global ice volume change than the planktonic δ^{18}O record [26]. In our study, the synchronous changes in Mg/Ca-SST and benthic δ^{18}O from Core SO18459 do not support the inference that surface seawater warming leads global ice volume change by ~3000 a [24]. Strictly speaking, the value of benthic δ^{18}O reflects only ~70% of high-latitude ice volume change or sea level change [16,26–28]. Therefore, it is difficult to estimate accurately the phase relationship between tropical surface seawater warming and high-latitude ice sheet melting based on proxy records from Core SO18459. The phase discrepancy between Mg/Ca-SST and benthic δ^{18}O could result from different transport rates of global eustatic signals in different ocean basins. In addition, unclear pathways of the δ^{18}O signal from the locus of deep water formation to the tropics also confound the correlation of benthic δ^{18}O and Mg/Ca-SST [5].

Comparison of the Mg/Ca-SST from Core SO18459 with the EDC3 δD and EDML (Figure 4) indicates that regional climate change in the tropical oceans is almost synchronous with climate change in the Antarctic. This implies a nearly instantaneous heat transfer between equatorial regions and the Antarctic at millennial timescales during Termination II. Because tropical oceans are important sources of global heat and water vapor transport, this in-phase relationship highlights the important role of tropical oceans in global climate change. The instantaneous heat transfer between low and high latitudes may occur via atmospheric teleconnection or thermohaline circulation. Visser et al. [3] suggested that changes in heat transport to the high southern latitudes may have been regulated by a system analogous to the El Niño/Southern Oscillation (ENSO). For example, the tropical Pacific was probably dominated by an El Niño-like climate during glacial period. At that time, the western Pacific SST decreased, the thermocline was shallow and air-sea exchange reduced. Conversely, a switch to La Niña-like conditions occurred during deglaciation and reinvigorated heat transport to high latitudes. Xu et al. [5] suggested that the synchronous changes in SST of the southern high latitudes and the tropical eastern Indian Ocean are probably caused by a direct and almost instantaneous atmospheric feedback through rapid transfer of heat by globally rising atmospheric CO_2 content.

3.2 YD-like events during Termination II

Cold events during deglaciation are good opportunities for studying the climate mechanism. According to the Milankovitch theory [29], solar radiation increases continuously during deglaciations. If climate change responds mainly to solar radiation, the cold events during deglaciations are thus hard to explain. However, the Younger Dryas (YD) cold event during the last deglaciation is observed widely in many records from both high and low latitudes. It is believed widely that the YD cold event was triggered by a flood of fresh water that poured into the north Atlantic and disrupted the thermohaline circulation [30,31]. Thus, on millennial timescales, besides solar radiation, the Earth's own internal system and feedback effects have a significant role in modulating global climate change.

However, cold events do not occur during all Pleistocene and earlier deglaciations. For example, the Younger Dryas-like (YD-like) cold event during the penultimate deglaciation is observed rarely in deep sea records from the global oceans. The oxygen isotopic records of stalagmites from Sanbao Cave [32] reveal YD-like (YD-III) and BA-like (BA-III) events in Termination III but not in Termination II and Termination IV.

In the Mg/Ca-SST record of Core SO18459, there is a YD-like cold event between ca. 130.5 and133.5 ka BP. The SST shows an abrupt decrease by ~0.8°C starting at ca. 133.5 ka BP and lasting for ~500 a. After that, the SST increases slowly and returns to the level before the YD-like event at ca. 130.5 ka BP. The SST increases rapidly then until ca. 130 ka BP, showing a warming of ~2.5°C over 500 a. Additionally, the YD-like cold event also occurs in the *G. ruber* δ^{18}O record, which shows an increase of ~0.35‰ between ca. 130.5 and 133.5 ka BP. The 0.8°C cooling during the YD-like event is equivalent to an increase of ~0.176‰ [33] in the planktonic δ^{18}O. The remaining ~0.174‰ increase in the planktonic δ^{18}O is caused by an increase in sea surface salinity. In the Timor Sea, rainfall brought by the Australian monsoon is an important factor influencing sea surface salinity. Therefore, weakening of the Australian monsoon may increase the sea surface salinity of the ITF. In addition, the strengthening of El Niño events can move the rainfall locus from the Western Pacific to the central Pacific. This leads to decreasing rainfall in the western Pacific and thus increasing sea surface salinity of the ITF, which then results in increased sea surface salinity in the Timor Sea.

The YD-like cold event has enhanced our understanding of the tropical climate system. Although the northward Australian winter monsoon changes rapidly to the East Asian summer monsoon, the two monsoonal systems retain their own characteristics. During Termination II, the increase in sea surface salinity in the Timor Sea indicates weakening of the Australian monsoon or strengthening of the El Niño events between ca. 130.5 and 133.5 ka BP. However, stalagmites oxygen isotopic records from Sanbao Cave [32] indicate that the East Asian summer monsoon did not weaken during the penultimate deglaciation. Therefore,

different climate systems from tropical regions may have different responses to El Niño events.

The YD-like cold event is also observed in the global benthic foraminiferal δ^{18}O records—LR04 [20] during Termination II, although it is not evident in the benthic δ^{18}O record of Core SO18459. The benthic δ^{18}O in LR04 increases from 3.67‰ at ca. 130 ka BP to 3.9‰ at ca. 129 ka BP, by as much as 0.23‰ (Figure 2). In Core MD01-2378, located nearby, a YD-like cold event is also observed in the benthic δ^{18}O record [4]. However, Antarctic ice core records such as the δ^{18}O of the EDML ice core and δD of the Dome C ice core do not record such YD-like cold events (Figure 4(c)). YD-like cold events observed in the benthic δ^{18}O records probably indicate amplification of the polar and continental ice sheets or temperature or salinity increases in deep seawater during deglaciation. The time resolution of the benthic δ^{18}O record of Core SO18459 is too low to reveal abrupt millennial-scale climate changes and neither does the benthic δ^{18}O record of LR04, which has higher time resolution. However, the YD-like cold event during Termination II as found in the benthic δ^{18}O of LR04 and in the climate proxy records in Cores SO18459 and MD01-2378 may indicate a teleconnection between high- and low-latitude climate changes.

4 Conclusion

The Mg/Ca-SST records of Core SO18459 in the Timor Sea indicate a 4.1°C warming of ITF over Termination II, which is in phase with decreasing planktonic and benthic δ^{18}O from the same core. Warming of the ITF and the Antarctic is nearly synchronous during Termination II, which indicates a nearly instantaneous heat transfer via the atmosphere or/and upper ocean between the equatorial regions and the Antarctic at millennial time scales. The *G. ruber* δ^{18}O and SST records of Core SO18459 show a marked YD-like cold event during Termination II, which is probably caused by a decrease in Australian monsoon-derived rainfall or strengthening of the Western Pacific Warm Pool. However, a similar YD-like cold event is not observed in East Asian rainfall records. This discrepancy indicates that different tropical climate systems may have different responses to the same forcing, such as the El Niño Southern Oscillation. A similar YD-like cold event is observed in global benthic foraminiferal δ^{18}O records during Termination II, implying a teleconnection of millennial-scale climate change between the tropical regions and the high latitudes.

This work was supported by the National Natural Science Foundation of China (40776028 and 40976024), the National Key Basic Research Special Foundation of China (2007CB815902) and the Foundation for the Author of National Excellent Doctoral Dissertation of China (2005036) and the Shanghai Rising-Star Program (10QH1402600), the Fok Ying Tong Education Foundation (111016) and the Program for New Century Excellent Talents in University (NCET-08-0401).

1 Rahmstorf S. Ocean circulation and climate during the past 120000 years. Nature, 2002, 419: 207–214
2 Pierrehumbert R. Climate change and the tropical Pacific: The sleeping dragon wakes. Proc Natl Acad Sci USA, 2000, 97: 1355–1358
3 Visser K, Thunell R, Stott L. Magnitude and timing of temperature change in the Indo-Pacific warm pool during deglaciation. Nature, 2003, 421: 152–155
4 Xu J, Kuhnt W, Holbourn A, et al. Changes in the vertical profile of the Indonesian Throughflow during Termination II: Evidence from the Timor Sea. Paleoceanography, 2006, 21: PA4202
5 Xu J, Holbourn A, Kuhnt W, et al. Changes in the thermocline structure of the Indonesian outflow during Terminations I and II. Earth Planet Sci Lett, 2008, 273: 152–162
6 Lea D, Pak D, Spero H. Climate impact of late Quaternary equatorial Pacific sea surface temperature variations. Science, 2000, 289: 1719–1924
7 Koutavas A, Lybch-Stieglitz J, Marchitto T M, et al. El Niño-like pattern in ice age tropical Pacific sea surface temperature. Science, 2002, 297: 226–230
8 Stott L, Timmerman A, Thunell R. Southern Hemisphere and deep-sea warming led deglacial atmospheric CO_2 rise and tropical warming. Science, 2007, 318: 435–438
9 Kienast M, Steinke S, Stattegger K, et al. Synchronous tropical South China Sea SST change and Greenland warming during deglaciation. Science, 2001, 291: 2132–2134
10 Gordon A L, Fine R A. Pathways of water between the Pacific and Indian oceans in the Indonesian seas. Nature, 1996, 379: 146–149
11 Martinet J I, Khan M E, Chivas A R, et al. New estimates for salinity changes in the Western Pacific Warm Pool during the Last Glacial Maximum: Oxygen-isotope evidence. Mar Micropaleontol, 1997, 32: 311–340
12 Martinez J I, Taylor L, De Deckker P, et al. Planktonic foraminifera from the eastern Indian Ocean: Distribution and ecology in relation to the Western Pacific Warm Pool (WPWP). Mar Micropaleontol, 1998, 34: 121–151
13 Kuhnt W, Holbourn A, Hall R, et al. Neogene history of the Indonesian Throughflow, in Continent-Ocean interactions within East Asia Marginal Seas. Geophys Monogr Ser, 2004, 149: 299–320
14 Tian J, Wang P, Cheng X, et al. Astronomically tuned Plio-Pleistocene benthic δ^{18}O record from South China Sea and Atlantic-Pacific comparison. Earth Planet Sci Lett, 2002, 203: 1015–1029
15 Vance D, Burton K. Neodymium isotopes in planktonic foraminifera: A record of the response of continental weathering and ocean circulation rates to climate change. Earth Planet Sci Lett, 1999, 173: 365–379
16 Shackleton N J. The 100000-year ice-age cycle identified and found to lag temperature, carbon dioxide, and orbital eccentricity. Science, 2000, 289: 1897–1902
17 Shackleton N J. Attainment of isotopic equilibrium between ocean water and the benthonic foraminifera genus uvigerina: Isotopic changes in the ocean during the last glacial. Les Meth Quant d'etude Var Clim Cours Pleist, Coll Int CNRS, 1974, 219: 203–209
18 Bemis B E, Spero H J, Bijma J, et al. Reevaluation of the oxygen isotopic composition of planktonic foraminifera: Experimental results and revised paleotemperature equations. Paleoceanography, 1998, 13: 150–160
19 Shackleton N J, Berger A, Peltier W R. An alternative astronomical calibration of the lower Pleistocene timescale based on ODP Site 677. Trans R Soc Edinburgh Earth Sci, 1990, 81: 251–261
20 Lisiecki L E, Raymo M E. A Pliocene-Pleistocene stack of 57 globally distributed benthic δ^{18}O records. Paleoceanography, 2005, 20: PA1003
21 Anand P, Elderfield H, Conte M H. Calibration of Mg/Ca thermometry in planktonic foraminifera from a sediment trap time series. Pa-

leoceanography, 2003, 18: 28–31
22 Dekens P S, Lea D W, Pak D K, et al. Core top calibration of Mg/Ca in tropical foraminifera: Refining paleotemperature estimation. Geochem Geophys Geosyst, 2002, 3, doi: 10.1029/2001GC000200
23 Waelbroeck C, Labeyrie L, Michel E, et al. Sea-level and deep water temperature changes derived from benthic foraminifera isotopic records. Quat Sci Rev, 2002, 21: 295–305
24 Lea D W, Pak D K, Belanger C L, et al. Paleoclimate history of Galápagos surface waters over the last 135000 years. Quat Sci Rev, 2006, 25: 1152–1167
25 EPICA Community Members. One-to-one coupling of glacial climate variability in Greenland and Antarctica. Nature, 2006, 444: 195–198
26 Billups K, Schrag D P. Paleotemperatures and ice volume of the past 27 Myr revisited with paired Mg/Ca and $^{18}O/^{16}O$ measurements on benthic foraminifera. Paleoceanography, 2002, 17, doi: 10.1029/2000PA000567
27 Skinner L C, Shackleton N J. An Atlantic lead over Pacific deep-water change across Termination I: Implications for the application of the marine isotope stage stratigraphy. Quat Sci Rev, 2005, 24: 571–580
28 Skinner L C, Shackleton N J. Deconstructing Terminations I and II: Revisiting the glacioeustatic paradigm based on deep-water temperature estimates. Quat Sci Rev, 2006, 25: 3312–3321
29 Milankovitch M. Mathematische Klimalehre und astronomishe Theorie der Klimasch-wankungen. In: Koppen W, Geiger R, eds. Handbuch der Klimatologie. Berlin: Gebruder Borntraeger, 1930. I: 1–76
30 Broecker W S. Does the trigger for abrupt climate change reside in the ocean or in the atmosphere? Science, 2003, 300: 1519–1522
31 Broecker W S. Was the Younger Dryas triggered by a flood? Science, 2006, 312: 1146–1148
32 Cheng H, Edwards R L, Broecker W S, et al. Ice Age terminations. Science, 2009, 326: 248–252
33 Wang L, Sarnthein M, Duplessy J-C, et al. Paleo sea surface salinities in the low-latitude Atlantic: The $\delta^{18}O$ record of *Globigerinoides Ruber* (white). Paleoceanography, 1995, 10: 749–761